Journal of the Egyptian Mathematical Society (2014) **22**, 123–133

Egyptian Mathematical Society

Journal of the Egyptian Mathematical Society

www.etms-eg.org
www.elsevier.com/locate/joems

ORIGINAL ARTICLE

Effects of temperature-dependent viscosity and variable thermal conductivity on MHD non-Darcy mixed convective diffusion of species over a stretching sheet

Dulal Pal [a,*], **Hiranmoy Mondal** [b]

[a] *Department of Mathematics, Siksha-Bhavana, Visva-Bharati University, Santiniketan, West Bengal 731 235, India*
[b] *Department of Mathematics, Bengal Institute of Technology and Management, Santiniketan, West Bengal 731 236, India*

Received 14 February 2013; revised 29 April 2013; accepted 21 May 2013
Available online 5 July 2013

KEYWORDS

Boundary layer flow;
Heat transfer;
Stretching surface;
Ohmic heating;
Non-Darcy flow

Abstract A numerical model is presented to study the effects of temperature-dependent viscosity and variable thermal conductivity on mixed convection problem. Two important types of wall heating conditions namely, prescribed surface temperature and prescribed wall heat flux which arise in polymer industries are considered. The problem is solved numerically by using the fifth-order Runge–Kutta Fehlberg method with shooting technique. It is found that the Prandtl number is to decrease the skin friction coefficient, local Nusselt number and local Sherwood number. The effects of non-uniform heat source/sink and porous parameter are analyzed on velocity, temperature, skin friction co-efficient, Nusselt and Sherwood numbers.

MATHEMATICS SUBJECT CLASSIFICATION: 65L10, 76D10, 76R10

1. Introduction

In recent years considerable attention has been shown on the study of thermal convection in porous media due to its rapid growth in the fluid mechanics research and its importance in petroleum and geothermal processes such as extrusion of plastic sheets, spinning of fibers, polymer sheet extruded continuously from a die and the cooling of metallic sheets in cooling bath. In mixed convection heat transfer takes place under conditions when there are large temperature differences within the fluid, it becomes necessary to consider variable fluid properties in such studies. Sparrow and Lee [1] analyzed the problem of mixed convection about a horizontal circular cylinder. Ali [2] considered the effect of temperature-dependent viscosity on mixed convection heat transfer along a moving surface. The effect of temperature-dependent viscosity and thermal radiation on MHD forced convection over a non-isothermal wedge was investigated by Pal and Mondal [3]. Many applications of convection in porous medium are provided in an excellent book by Nield and Bejan [4]. Abel and Mahesha

* Corresponding author. Tel.: +91 3463 261029.
E-mail addresses: dulalp123@rediffmail.com (D. Pal), hiranmoymondal@yahoo.co.in (H. Mondal).

Peer review under responsibility of Egyptian Mathematical Society.

ELSEVIER Production and hosting by Elsevier

1110-256X © 2013 Production and hosting by Elsevier B.V. on behalf of Egyptian Mathematical Society. Open access under CC BY-NC-ND license.
http://dx.doi.org/10.1016/j.joems.2013.05.010

Nomenclature

A	parameters of temperature distribution on the stretching surface
B	parameter of mass distribution on the stretching surface
b	stretching parameter
$\vec{B}$	transverse magnetic field
B_0	uniform transverse magnetic field
C	concentration of the species
C_f	local skin-friction coefficient
C_p	Specific heat at constant pressure
D	mass diffusion coefficient
$\vec{E}$	electric field
E_c	Eckert number
E_0	uniform electric field
E_1	local electromagnetic parameter
F^*	local inertia-coefficient
g	acceleration due to gravity
Ha	Hartmann number
k	permeability of the porous medium
k_1	porous parameter
Nr	thermal radiation parameter
Pr	Prandtl number
q_s	radiative heat flux in the y-direction
Re_x	local Reynolds number
Sc	Schmidt number
Sh_x	local Sherwood number
T	temperature of the fluid
T_w	stretching sheet temperature
T_∞	temperature far away from the stretching sheet
u	velocity of the fluid in the x-direction
v	velocity of the fluid in the y-direction
x	flow directional coordinate along the stretching sheet
y	distance normal to the stretching sheet

Greek symbols

θ	non-dimensional temperature parameter
β_T	co-efficient of thermal expansion
β_C	volumetric co-efficient of expansion with concentration
η	similarity variable
ν	kinematic viscosity
ρ	density of the fluid
κ	thermal conductivity
δ	solutal buoyancy parameter
σ	magnetic permeability
σ_s	Stefan-Boltzmann constant
λ	buoyancy parameter or mixed convection parameter

[5] analyzed the heat transfer in MHD viscoelastic fluid flow over a stretching sheet with variable thermal conductivity, non-uniform heat source and radiation.

In many cases, porous media with high permeability, the viscous effects due to frictional drag at the boundary and the inertia effects within a porous medium become significant (see Chen and Lin [6]). Tong and Subramanium [7] considered Brinkmann-extended Darcy model to examine the buoyancy effects on free convection in a vertical cavity. Tien and Hunt [8] analyzed non-Darcian effects for a boundary layer flow and heat transfer in porous beds. Singh and Tewari [9] analyzed the effects of thermal stratification on free convection flow in order to study the effects of inertia by considering non-Darcy model. Kazem et al. [10] improved analytical solutions to a stagnation-point flow past a porous stretching sheet with heat generation. Uddin and Kumar [11] analyzed the effect of temperature– dependent properties on MHD free convection flow and heat transfer near the lower stagnation point of a porous isothermal cylinder. The unsteady convective boundary layer flow of a viscous fluid at a vertical surface with variable fluid properties was studied by Vajravelu et al. [12]. The effects of thermal radiation and variable fluid viscosity on stagnation point flow past a porous stretching sheet was studied by Mukhopadhyay [13]. Recently, Mahantesh et al. [14] analyzed the MHD flow and heat transfer over a stretching surface with variable thermal conductivity and partial slip.

A considerable interest has been shown in the study of thermal radiation on convection for heat and mass transfer in fluids due to its significant effects in the surface heat transfer. Further, thermal radiation effects on flow and heat transfer processes are of major importance in the space technology and high temperature processes. Also, the effect of thermal radiation play a significant role in controlling heat transfer in the production of quality product as it depends on the heat controlling factor. Ali et al. [15] have examined natural convection-radiation interaction in boundary layer flow over semi-infinite horizontal surface. Pal [16] investigated heat and mass transfer in stagnation-point flow in viscous fluid over a stretching vertical sheet by considering buoyancy force and thermal radiation. Bataller [17] studied the effects of thermal radiation on the Blasius flow. Later, Magyari and Pantokratoras [18] examined the effect of thermal radiation using in the linearized Rosseland approximation on the heat transfer characteristics in boundary layer flow. Pal and Mondal [19] analyzed combined effects of thermal radiation and heat generation on convection heat transfer of an optically dense viscous incompressible fluid over a vertical surface embedded in a fluid saturated porous medium of variable porosity. EL-Kabeir [20] studied Soret and Dufour effects on heat and mass transfer mixed convection over a vertical surface saturated porous medium. The convective radiation effect from a continuously moving fin of variable thermal conductivity analyzed by Abdul Aziz and Khani [21]. The effect of variable viscosity on mixed convection heat transfer along a vertical moving surface analyzed by Mohamed Ali [22]. Hussain et al. [23] studied the radiation effects on the thermal boundary layer flow of a micropolar fluid towards a permeable stretching sheet. Mohamed Abd El-Aziz [24] studied the temperature dependent viscosity and thermal conductivity effects on combined heat and mass transfer in MHD three-dimensional flow over a stretching surface with Ohmic heating. Ramesh et al. [25] studied the MHD flow of a dusty fluid near the stagnation point over a permeable stretching sheet with non-uniform source/sink. Sivaraj and Rushi Kumar [26] analyzed the viscoelastic

fluid flow over a moving vertical cone and flat plate with variable electric conductivity.

The main purpose of this study is to examine the effects of non-uniform heat source/sink, temperature-dependent viscosity and variable thermal conductivity on mixed convection boundary layer flow, heat and mass transfer over a stretching sheet in a porous medium in the presence of thermal radiation, and Ohmic heating due to magnetic field as well as electric field. We have adopted two different types of boundary heating conditions namely, the prescribed surface temperature (PST) and the prescribed surface heat flux (PHF), respectively. The non-linearity governing basic equations have led us to adopt numerical solution of the coupled ordinary differential equations. The Darcy–Forchheimer model is used to describe the fluid flow in the porous medium. Highly non-linear momentum and heat transfer equations are solved numerically using fifth-order Runge–Kutta Fehlberg method with shooting technique (Na, [27]). The effects of Prandtl number, porous parameter and non-uniform heat source/sink are analyzed on the velocity, temperature and concentration profiles as well as on local skin-friction co-efficient, local Nusselt number and local sherwood number are presented in graphical and in tabular form. It is hoped that the results obtained from the present investigation will provide useful information for various industrial applications. Moreover, the temperature profiles decreases with the increase in the variable viscosity parameter, while it decreases with the increase in variable thermal conductivity parameter.

2. Mathematical formulations

We have considered two-dimensional steady incompressible electrically conducting fluid flow over a continuous stretching sheet embedded in a porous medium. The flow region is exposed under uniform transverse magnetic fields $\overrightarrow{B_0} = (0, B_0, 0)$ and uniform electric field $\overrightarrow{E} = (0, 0, -E_0)$. Since such imposition of electric and magnetic fields stabilizes the boundary layer flow. It is assumed that the flow is generated by stretching of an elastic sheet from a slit by imposing two equal and opposite forces in such a way that velocity of the sheet is of linear order of the flow direction. (see Fig. 1). We know from Maxwell's equation that $\nabla.\overrightarrow{B} = 0$ and $\nabla \times \overrightarrow{E} = 0$. When magnetic field is not so strong then electric field and magnetic field obey Ohm's law $\overrightarrow{J} = \sigma(\overrightarrow{E} + \vec{q} \times \overrightarrow{B})$, where $\overrightarrow{J}$ is the Joule current. The induced magnetic field is assumed to be small. The viscous dissipation and velocity of the fluid far away from the plate are assumed to be negligible. The fluid properties are assumed to be isotropic and constant, except for the fluid viscosity μ which is assumed to vary as an inverse linear function of temperature T, in the form (see Lai and Kulacki [28]):

$$\frac{1}{\mu} = \frac{1}{\mu_\infty}[1 + \gamma(T - T_\infty)] \tag{1}$$

or

$$\frac{1}{\mu} = a(T - T_r) \tag{2}$$

where

$$a = \frac{\gamma}{\mu_\infty} \quad and \quad T_r = T_\infty - \frac{1}{\gamma} \tag{3}$$

Both a and T_r are constant and their values depend on the reference state and the thermal property of the fluid, i.e. γ. In general, $a > 0$ for liquids and $a < 0$ for gases. Consider the uniform flow of fluid with velocity U_w through a porous medium bounded by a semi-infinite flat plate parallel to the flow. Also, θ_r is a constant which is defined by

$$\theta_r = \frac{T_r - T_\infty}{T_w - T_\infty} = -\frac{1}{\gamma(T_w - T_\infty)} \tag{4}$$

It is worth mentioning here that for $\gamma \to 0$, i.e. $\mu = \mu_\infty$ (constant) then $\theta_r \to \infty$. It is also important to note that θ_r is negative for liquids and positive for gases.

The flow model is based on the assumption that the flow is steady, incompressible, laminar and the fluid viscosity which is assumed to be an inverse linear function of temperature. The fluid is assumed to be Newtonian and its property variations due to temperature are limited to density and viscosity. We take into account of uniform magnetic field as well as electric field effects in the momentum and thermal boundary layer equations. Under the usual boundary layer approximation, the governing equations describing the conservation of mass, momentum, energy and concentration in the presence of radiation magnetic field and non-uniform heat source/sink can be written as [19]:

Continuity equation:

$$\frac{\partial u}{\partial x} + \frac{\partial v}{\partial y} = 0 \tag{5}$$

Momentum equation:

$$\frac{1}{\phi^2}\left(u\frac{\partial u}{\partial x} + v\frac{\partial u}{\partial y}\right) = \frac{1}{\rho_\infty \phi}\frac{\partial}{\partial y}\left(\mu\frac{\partial u}{\partial y}\right) + \frac{\sigma}{\rho_\infty}\left(E_0 B_0 - B_0^2 u\right) - \frac{v}{k}u - \frac{C_b}{\sqrt{k}}u^2 + g_t\beta_T(T - T_\infty) + g_t\beta_C(C - C_\infty) \tag{6}$$

Energy equation:

$$\rho_\infty C_p\left(u\frac{\partial T}{\partial x} + v\frac{\partial T}{\partial y}\right) = \frac{\partial}{\partial y}\left(\kappa\frac{\partial T}{\partial y}\right) + q''' - \frac{\partial q_s}{\partial y} + \sigma(uB_0 - E_0)^2 \tag{7}$$

Conservation of species:

$$u\frac{\partial C}{\partial x} + v\frac{\partial C}{\partial y} = D\frac{\partial^2 C}{\partial y^2} \tag{8}$$

where u and v are the velocity components in the x and y directions, respectively; v_∞ is the kinematic viscosity; g_t is the acceleration due to gravity; ρ_∞ is the density of the fluid; β_T is the coefficient of thermal expansion; β_C is the volumetric coefficient of expansion with concentration, T is the temperature of the

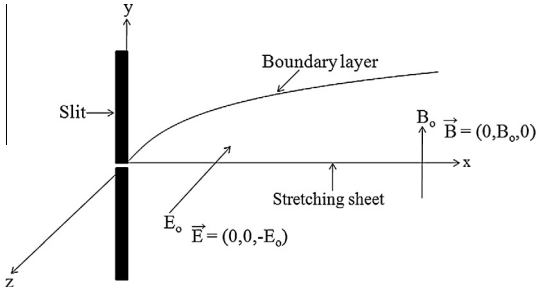

Figure 1 Boundary layer over stretching sheet.

fluid inside the thermal boundary layer and T_∞ is the fluid temperature in the free stream. k is the permeability of the porous medium; ϕ is the porosity of the porous medium; C_b is the form of drag coefficient which does not depends on the viscosity and other physical properties of the fluid depends on the geometry of the medium. T is the temperature of the liquid, C is the concentration of the species, D is the diffusion coefficient, ρ is the density of the liquid, C_p is the specific heat at constant pressure and κ is the thermal conductivity. Thermal boundary layer takes into account the Ohmic dissipation due to the magnetic and electric fields. The thermal conductivity κ is assumed to vary linearly with temperature which is of the form

$$\kappa = \kappa_\infty[1+\epsilon\theta(\eta)] \text{ in PST case,}$$
$$\text{and} \quad \kappa = \kappa_\infty[1+\epsilon g(\eta)] \text{ in PHF case}$$

where

$$\theta(\eta) = g(\eta) = \frac{T-T_\infty}{T_w-T_\infty}, \quad \text{and} \quad H(\eta) = \frac{C-C_\infty}{C_w-C_\infty} \tag{9}$$

and ϵ is a small parameter. The non-uniform heat source/sink q''' is modeled as

$$q''' = \frac{\kappa U_w(x)}{xv}[A_s(T_w-T_\infty)e^{-\eta} + (T-T_\infty)B_s], \tag{10}$$

where A_s and B_s are the coefficients of space and temperature-dependent heat source/sink, respectively. Here we make a note that, the case $A_s > 0$, $B_s > 0$ corresponds to internal heat generation and that $A_s < 0$, $B_s < 0$ corresponds to internal heat absorption. Following Rosseland approximation the radiative heat flux q_s is modeled as,

$$q_s = -\frac{4\sigma_s}{3k_s}\frac{\partial T^4}{\partial y}, \tag{11}$$

where σ_s is the Stefan–Boltzmann constant and k_s is the mean absorption coefficient. Let us introduce the wall temperature excess ratio parameter $\theta_w = \frac{T_w}{T_\infty}$ (Pal and Mondal [29]). Thus using (9), T^4 may be expressed as

$$T^4 = T_\infty^4\{1+(\theta_w-1)\theta\}^4 \tag{12}$$

The following appropriate boundary conditions on velocity are employed to include the effect of stretching of the boundary surface causing flow in the x-direction as

$$\begin{aligned} &u = U_w(x) = bx, \quad v = 0 \quad at\ y = 0 \\ &u = 0 \quad as\ y \to \infty \end{aligned} \tag{13}$$

To solve the governing boundary layer Eqs. (3), (4) and (10) the following similarity transformations are introduced

$$u = bxf'(\eta), \quad v = -\sqrt{bv_\infty}f(\eta) \quad \eta = \sqrt{\frac{b}{v_\infty}}y \tag{14}$$

Substitution of Eq. (14) in Eq. (6) results in a third-order nonlinear ordinary differential equation of the following form

$$\begin{aligned} &f''' + \frac{1}{\theta_r-\theta}\theta' f'' - \phi k_1 f' \\ &+ \left(1-\frac{\theta}{\theta_r}\right)\left[\frac{ff''}{\phi} - \frac{f'^2}{\phi} + \phi\{Ha^2(E_1-f') - F^* f'^2 + \lambda\theta + \delta H\}\right] \\ &= 0 \end{aligned} \tag{15}$$

where $k_1 = \frac{v_\infty}{kb}$ is the porous parameter, $Ha = \sqrt{\frac{\sigma}{\rho_\infty b}}B_0$ is Hartmann number, $E_1 = \frac{E_0}{B_0 bx}$ is the local electric parameter, $F^* = \frac{C_b}{\sqrt{k}}x$ is the local inertia-coefficient, $\lambda = \frac{Gr_x}{Re_x^2}$ is the buoyancy or mixed convection parameter, $Gr_x = \frac{g_t\beta_T(T_w-T_\infty)x^3}{v_\infty^2}$ is the local Grashof uumber, $\delta = \frac{Gr_c}{Re_x^2}$ is the buoyancy or mixed convection parameter with species, $Gr_c = \frac{g_t\beta_c(C-C_\infty)}{b^2 l}$ is solutal Grashof number, ϕ is the porosity of the porous medium and $Re_x = \frac{U_w x}{v_\infty}$ is the local Reynolds number.

In view of the above similarity transformations, the boundary conditions (13) take the following form:

$$f(0) = 0,\ f'(0) = 1,\ f'(\infty) = 0. \tag{16}$$

The important physical quantities of interest are the skin-friction coefficient, C_f, which is defined as

$$C_f = \frac{\tau_w}{\rho U_w^2/2}, \tag{17}$$

and wall sharing stress τ_w appeared in Eq. (17) is given by

$$\tau_w = \mu\left(\frac{\partial u}{\partial y}\right)_{y=0}. \tag{18}$$

After using the non-dimensional variables given by (14), we finally get the skin-friction coefficient as follows:

$$\frac{1}{2}C_f Re_x^{1/2} = \frac{\theta_r}{\theta_r-\theta}f''(0). \tag{19}$$

where $Re_x = \frac{xU_w(x)}{v_\infty}$ is the local Reynolds number.

2.1. PST Case

To solve the thermal boundary layer and concentration Eqs. (10) and (5), we consider non-isothermal temperature and concentration boundary conditions as follows:

$$\begin{aligned} &T = T_w = T_\infty + A\left(\frac{x}{l}\right)^2,\ C = C_w = C_\infty + B\left(\frac{x}{l}\right)^2 \quad \text{at } y = 0 \\ &T \to T_\infty, \quad C \to C_\infty \quad \text{as } y \to \infty \end{aligned} \tag{20}$$

where A and B is the parameters of temperature and concentration distribution on the stretching surface, l is the characteristic length.

We introduce a dimensionless temperature and concentration variable

$$\theta(\eta) = \frac{T-T_\infty}{T_w-T_\infty}, \quad H(\eta) = \frac{C-C_\infty}{C_w-C_\infty},$$

where

$$T-T_\infty = A\left(\frac{x}{l}\right)^2\theta(\eta), \quad C-C_\infty = B\left(\frac{x}{l}\right)^2 H(\eta) \tag{21}$$

We obtain the following non-linear ordinary differential equation for $\theta(\eta)$ and $H(\eta)$ as

$$\begin{aligned} &[((1+\epsilon\theta) + Nr\{1+(\theta_w-1)\theta\}^3)\theta']' + \left(1-\frac{\theta}{\theta_r}\right) \\ &Pr[(f\theta' - 2f'\theta) + Ha^2 E_c(E_1-f')^2] + \left(1-\frac{\theta}{\theta_r}\right) \\ &(1+\epsilon\theta)(A_s e^{-\eta} + B_s\theta) = 0 \end{aligned} \tag{22}$$

$$H'' + Sc(fH' - 2f'H) = 0 \tag{23}$$

where $Pr = \frac{\mu_\infty C_p}{k_\infty}$ is the Prandtl number, $E_c = \frac{b^2 l^2}{AC_p}$ is the Eckert number, $Nr = \frac{16\sigma^* T_\infty^3}{3k_\infty k^*}$ is the thermal radiation and $Sc = \frac{v_\infty}{D}$ is the Schmidt number.

Corresponding thermal boundary conditions become

$$\theta(\eta) = 1, \quad H(\eta) = 1 \quad \text{at } \eta = 0,$$
$$\theta(\eta) \to 0, \quad H(\eta) \to 0 \quad \text{as } \eta \to \infty. \tag{24}$$

The local Nusselt number which are defined as

$$Nu_x = \frac{xq_w}{\kappa(T_w - T_\infty)} \tag{25}$$

where q_w is the heat transfer from the sheet is given by

$$q_w = -\left[\left(\frac{16\sigma^* T^3}{3k^*} + \kappa\right)\frac{\partial T}{\partial y}\right]_{y=0} \tag{26}$$

Using the non-dimensional variables (20) and (21), we get from Eqs. (25) and (26) as

$$Nu_x/Re_x^{1/2} = -(1 + Nr\theta_w^3)\theta'(0) \tag{27}$$

The local Sherwood number which is defined as

$$Sh_x = \frac{xq_m}{D(C_w - C_\infty)} \tag{28}$$

where

$$q_m = -D\left(\frac{\partial C}{\partial y}\right)_{y=0} \tag{29}$$

Using the non-dimensional variables (20) and (21), we get from Eqs. (28) and (29) as

$$Sh_x/Re_x^{1/2} = -H'(0) \tag{30}$$

2.2. PHF Case

The boundary conditions in case of prescribed power law heat flux is of the form

$$-\kappa_\infty \frac{\partial T}{\partial y} = q_w = E\left(\frac{x}{l}\right)^2, \quad -\kappa_\infty \frac{\partial C}{\partial y} = q_m = F\left(\frac{x}{l}\right)^2 \text{ at } y = 0,$$
$$T \to T_\infty, \quad C \to C_\infty \text{ as } y \to \infty, \tag{31}$$

where E, F is a constant and $\kappa = \kappa_\infty[1 + \epsilon g(\eta)]$ (for energy) and $\kappa = \kappa_\infty[1 + \epsilon I(\eta)]$ (for concentration). Now we define the non-dimensional temperature $g(\eta)$ and concentration $I(\eta)$ as

$$g(\eta) = \frac{T - T_\infty}{T_w - T_\infty}, \quad I(\eta) = \frac{C - C_\infty}{C_w - C_\infty}$$
$$T - T_\infty = \frac{E}{\kappa_\infty}\left(\frac{x}{l}\right)^2\sqrt{\frac{\nu_\infty}{b}}g(\eta), \quad C - C_\infty = \frac{F}{\kappa_\infty}\left(\frac{x}{l}\right)^2\sqrt{\frac{\nu_\infty}{b}}I(\eta)$$

where

$$T_w - T_\infty = \frac{E}{\kappa_\infty}\left(\frac{x}{l}\right)^2\sqrt{\frac{\nu_\infty}{b}}, \; C_w - C_\infty = \frac{F}{\kappa_\infty}\left(\frac{x}{l}\right)^2\sqrt{\frac{\nu_\infty}{b}} \tag{32}$$

Using Eqs. (31) and (32) in Eqs. (7) and (8), we obtain the non-linear ordinary differential equation for $g(\eta)$ and $I(\eta)$ in the form

$$\left[((1 + \epsilon g) + Nr\{1 + (g_w - 1)g\}^3)g'\right]' + \left(1 - \frac{g}{g_r}\right)$$
$$Pr[(fg' - 2f'g) + Ha^2E_s(E_1 - f')^2] + \left(1 - \frac{g}{g_r}\right)$$
$$(1 + \epsilon g)(A_s e^{-\eta} + B_s g) = 0 \tag{33}$$
$$I'' + Sc(fI' - 2f'I) = 0. \tag{34}$$

where $E_s = E_c k_\infty \sqrt{\frac{b}{\nu_\infty}}$ is the scaled Eckert number. Corresponding thermal boundary conditions for $g(\eta)$ and $I(\eta)$ are given by

$$g'(\eta) = -1, \quad I'(\eta) = -1 \quad \text{at} \quad \eta = 0$$
$$g(\eta) \to 0, \quad I(\eta) \to 0 \quad \text{as} \quad \eta \to \infty \tag{35}$$

3. Numerical Method

The coupled ordinary differential Eqs. (15), (22), (23), (33) and (34) are of third order in f, and second order in θ and H which have been reduced to a system of seven simultaneous equations of first-order for seven unknowns. In order to solve this system of equations numerically we require seven initial conditions but two initial conditions on f and one initial condition each on θ and H are known. However, the values of f', θ and H are known at $\eta \to \infty$. Thus, these three end conditions are utilized to produce three unknown initial conditions at $\eta = 0$ by using shooting technique. The most crucial factor of this scheme is to choose the appropriate finite value of η_∞. Thus to estimate the value of η_∞, we start with some initial guess value and solve the boundary value problem consisting of Eqs. (15), (22), (23), (33) and (34) to obtain $f''(0)$, $\theta'(0)$ and $H'(0)$. The solution process is repeated with another large value of η_∞ until two successive values of $f''(0)$,$\theta'(0)$ and $H'(0)$ differ only after desired significant digit. The last value of η_∞ is taken as the finite value of the limit $\eta \to \infty$ for a particular set of physical parameters for determining velocity $f(\eta)$, temperature $\theta(\eta)$ and concentration $H(\eta)$ in the boundary layer. After knowing all the five initial conditions we solve this system of simultaneous equations using fifth-order Runge–Kutta–Fehlberg integration scheme with automatic generation of grid size so that convergence can be achieved at a faster rate. Thus, the coupled non-linear boundary value problem of third-order in f, second-order in θ and H has been reduced to a system of seven simultaneous equations of first-order for seven unknowns as follows:

$$f_1' = f_2, \quad f_2' = f_3,$$
$$f_3' = -\frac{1}{\theta_r - f_4}f_5 f_3 + \phi k_1$$
$$f_2 - \left(1 - \frac{f_4}{\theta_r}\right)\left[\frac{f_1 f_3}{\phi} - \frac{f_2^2}{\phi} + \phi\{Ha^2(E_1 - f_2) - F^* f_2^2 + \lambda f_4 + \delta f_6\}\right]$$
$$f_4' = f_5 \tag{36}$$

$$f_5' = -\frac{1}{(1 + \epsilon f_4) + Nr\{1 + (\theta_w - 1)f_4\}^3}$$
$$\times \left[\left(\epsilon + 3Nr(\theta_w - 1)\{1 + (\theta_w - 1)f_4\}^2\right)f_5^2\right.$$
$$+ \left(1 - \frac{f_4}{\theta_r}\right)Pr[(f_1 f_5 - 2f_2 f_4) + Ha^2 Ec(E_1 - f_2)^2$$
$$\left.+(1 + \epsilon f_4)(A_s e^{-\eta} + B_s f_4)]\right]$$
$$f_6' = f_7, \quad f_7' = -Sc(f_1 f_7 - 2f_2 f_6) \tag{37}$$

where

$$f_1 = f, \quad f_2 = f', \quad f_3 = f'', \quad f_4 = \theta, \quad f_5 = \theta', \quad f_6 = H, \; f_7 = H'$$

and a prime denotes differentiation with respect to η.

The boundary conditions now become

$$f_1 = 0, \quad f_2 = 1, \quad f_4 = 1, \quad f_6 = 1, \quad at \quad \eta = 0$$
$$f_2 \to \infty, \quad f_4 \to 0, \quad f_6 \to 0 \quad as \quad \eta \to \infty \tag{38}$$

Since $f_3(0)$, $f_5(0)$ and $f_7(0)$ are not prescribed so we have to start with the initial approximations as $f_3(0) = s_{10}$, $f_5(0) = s_{20}$ and $f_7(0) = s_{30}$. Let γ_1, γ_2 and γ_3 be the correct values of $f_3(0)$, $f_5(0)$ and $f_7(0)$, respectively. The resultant system of seven ordinary differential equations is integrated using fifth-order Runge–Kutta–Fehlberg method and denote the values of f_3, f_5 and f_7 at $\eta = \eta_\infty$ by $f_3(s_{10}, s_{20}, s_{30}, \eta_\infty)$, $f_5(s_{10}, s_{20}, s_{30}, \eta_\infty)$ and $f_7(s_{10}, s_{20}, s_{30}, \eta_\infty)$, respectively. Since f_3, f_5 and f_7 at $\eta = \eta_\infty$ are clearly function of γ_1, γ_2 and γ_3, they are expanded in Taylor series around $\gamma_1 - s_{10}$, $\gamma_2 - s_{20}$ and $\gamma_3 - s_{30}$, respectively by retaining only the linear terms. The use of difference quotients is made for the derivatives appeared in these Taylor series expansions. Thus, after solving the system of Taylor series expansions for $\delta\gamma_1 = \gamma_1 - s_{10}$, $\delta\gamma_2 = \gamma_2 - s_{20}$ and $\delta\gamma_3 = \gamma_3 - s_{30}$, we obtain the new estimates $s_{11} = s_{10} + \delta s_{10}$, $s_{21} = s_{20} + \delta s_{20}$ and $s_{31} = s_{30} + \delta s_{30}$. Next the entire process is repeated starting with $f_1(0), f_2(0), s_{11}, f_4(0), s_{21}$ and s_{31} as initial conditions. Iteration of the whole outlined process is repeated with the latest estimates of γ_1, γ_2 and γ_3 until prescribed boundary conditions are satisfied.

Finally, $s_{1n} = s_{1(n-1)} + \delta s_{1(n-1)}$, $s_{2n} = s_{2(n-1)} + \delta s_{2(n-1)}$ and $s_{3n} = s_{3(n-1)} + \delta s_{3(n-1)}$ for $n = 1, 2, 3, \ldots$ are obtained which seemed to be the most desired approximate initial values of $f_3(0), f_5(0)$ and $f_7(0)$. In this way all the six initial conditions are determined. Now it is possible to solve the resultant system of seven simultaneous equations by fifth-order Runge–Kutta–Fehlberg integration scheme so that velocity, temperature fields and concentration for a particular set of physical parameters can easily be obtained. The results are provided in several tables and graphs.

4. Results and discussion

Numerical solutions for the effects of thermal radiation on non-Darcy mixed convection heat transfer over a stretching sheet with variable thermal conductivity and temperature-dependent viscosity are investigated in presence of thermal radiation and non-uniform heat source/sink. The set of highly non-linear ordinary differential Eqs. (15), (22), (23), (33) and (34) subject to the boundary conditions (16), (24) and (35) constitute a two-point boundary value problem, which is integrated by fifth order Runge–Kutta Fehlberg method with shooting technique. In this method it is important to choose the appropriate finite values of $\eta \to \infty$. In order to verify the validity and accuracy of the present analysis, results for heat transfer $-\theta'(0)$ were compared with those reported by Grubka and Bobba [30] for some limiting conditions. The comparison in the above cases is found to be in excellent agreement, as shown in Table 1. The values of local skin-friction coefficient, local Nusselt number and local Sherwood number are tabulated in Table 2 for various values of local inertia coefficient F^*, solutal buoyancy parameter δ, Hartmann number Ha, temperature dependent viscosity parameter θ_r and thermal radiation parameter Nr. It is noted that the values of the local Nusselt number and local Sherwood number decreses and increase in the local skin friction coefficient by increasing the local inertia coefficient and Hartmann number. It is also found that the local Nusselt number and local Sherwood number increases with increase in the buoyancy and viscosity parameter but decreases the local skin friction coefficient. It is also pointed out from this table that increasing the values of thermal radiation parameter is to rise in the values of local Sherwood number whereas reverse trend is seen for local Nusselt number and local skin-friction coefficient. The effect of various physical parameters such as buoyancy parameter, porous parameter, space-dependent and temperature-dependent heat source/sink parameter on velocity, temperature and concentration profiles in PST case and PHF cases are shown in Figs. 2–16.

Table 1 Comparison of wall temperature gradient $-\theta'(0)$ for various values of Pr for $Ha = E_1 = E_c = A_s = B_s = \epsilon = \phi = k_1 = F^* = \lambda = Nr = Sc = 0.0$, $\theta_r \to \infty$, $\phi = 1$ with Grubka and Bobba [30].

Pr	Grubka and Bobba [30]	Present results
0.72	1.0885	1.088548
1.00	1.3333	1.353545
3.0	2.5097	2.507866
10.0	4.7969	4.795510

Fig. 2 represents the variations of velocity distribution in the boundary layer for various values of mixed convection parameter or buoyancy parameter λ. It is observed from this figure that the velocity distribution increases with increasing the buoyancy parameter λ, this is due to the fact that the boundary layer thickness increases with λ.

Fig. 3 represents the variation of temperature distribution in the boundary layer for various values of mixed convection parameter or buoyancy parameter λ. It is observed from these figures that the temperature distribution decreases with increasing the buoyancy parameter λ due to the reason that the thermal boundary layer thickness decreases with increase in the buoyancy parameter.

Fig. 4 represents the variations of velocity profiles in the boundary layer for various values of porous parameter k_1. It is observed from these figure that the velocity distribution decreases with increasing the porous parameter k_1. This is due to increase in the obstruction of the fluid motion with increase in the porous parameter (since permeability of the porous medium appears in the denominator of the porous parameter), thereby increase in the porous parameter indicates decreases in the permeability of the porous medium so the fluid velocity decreases.

The variation of temperature profiles $\theta(\eta)$ in the thermal boundary layer in presence of porous parameter k_1 is depicted in Fig. 5. It is found that the effect of porous parameter is to increase the temperature profile due to the fact that the increase in porous parameter k_1 decreases permeability which results in obstruction in the motion of the fluid due to which there is increase in the temperature in the thermal boundary layer. In other words, temperature increases with increase in the porous parameter due to the resistance offered to the fluid motion in the form of Darcy drag produced by the porous medium.

Fig. 6 depicts the effects of non-uniform heat generation A_s, $B_s > 0$ or absorption A_s, $B_s < 0$ parameter on the temperature distribution. It is observed that there is generation of energy in the thermal boundary layer by increasing the values of A_s, $B_s > 0$ (heat source) which causes the temperature of the fluid to increase, which in turn results in further increase of the flow field due to the thermal buoyancy effect. This is the main reason behind the temperature profiles to increase, whereas in the

Table 2 Value of Skin-friction coefficient, Nusselt number and Sherwood number for different parameters $\epsilon = 0.2$, $\phi = 0.6$, $Gc = 0.2$, $E_1 = 0.2$, $k1 = 0.2$, $\lambda = 2.0$, $Pr = 10.0$, $As = -2.0$, $Bs = -2.0$, $E_c = 0.2$, $Sc = 0.22$, $\theta_w = 1.2$.

F^*	δ	Ha	θ_r	Nr	$C_f Re_x^{1/2}$	$Nu_x Re_x^{-1/2}$	$Sh_x Re_x^{-1/2}$
0.5	0.5	0.2	−4.0	0.2	−1.275190	4.464208	0.5029314
1.2					−1.394402	4.448461	0.4954417
2.0					−1.521640	4.431759	0.4876322
1.2	0.5	0.2	−4.0	0.2	−1.394402	4.448461	0.4954417
	1.2				−1.150537	4.484265	0.5378202
	2.0				−0.9084269	4.519088	0.5754539
1.2	2.0	0.2	−2.0	0.2	−1.032235	4.806014	0.5727843
		1.2			−1.290083	4.564397	0.5605545
		2.0			−1.704449	4.182478	0.5380874
1.2	2.0	1.2	−4.0	0.2	−1.132555	4.288551	0.5591856
			−2.0		−1.290083	4.564397	0.5605545
			2.0		−0.8943129	5.430748	0.6191786
1.2	2.0	1.2	−4.0	0.2	−1.132555	4.288551	0.5591856
				1.2	−1.056634	2.837676	0.5669879
				2.0	−1.015118	2.343448	0.5694407

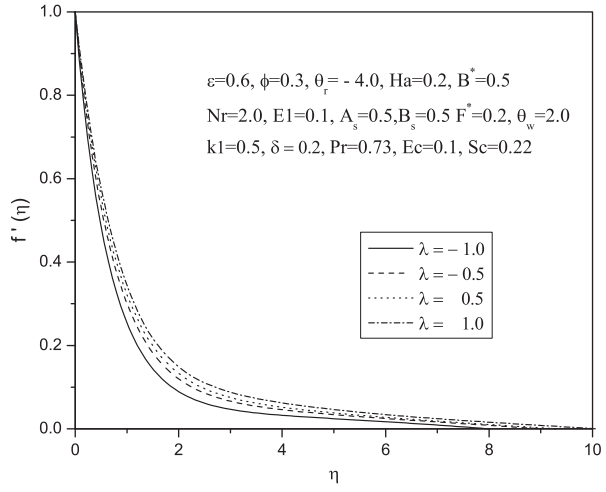

Figure 2 Variation of $f'(\eta)$ on buoyancy parameter λ.

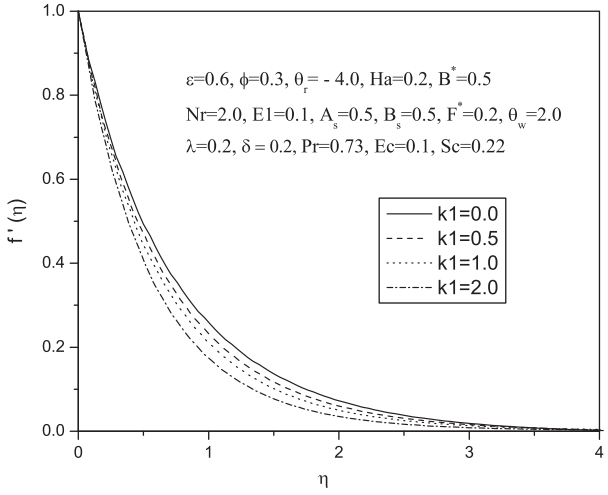

Figure 4 The variations of $f'(\eta)$ on porous parameter k_1.

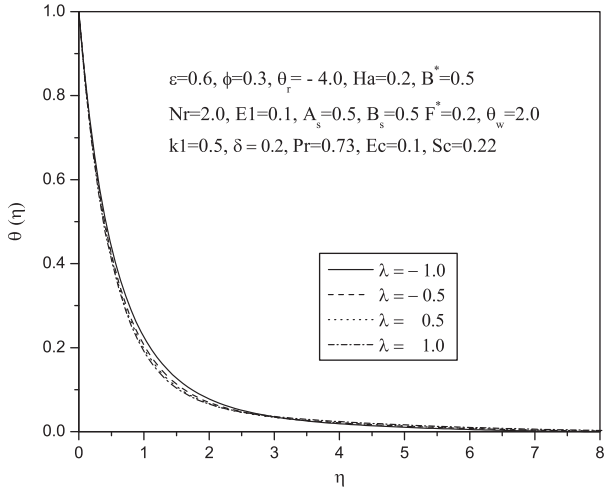

Figure 3 Effect of λ on the temperature profile in PST case.

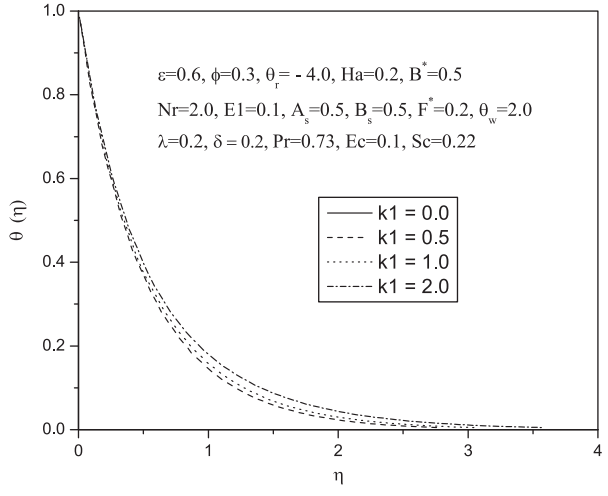

Figure 5 Effect of k_1 on the temperature profile in PST case.

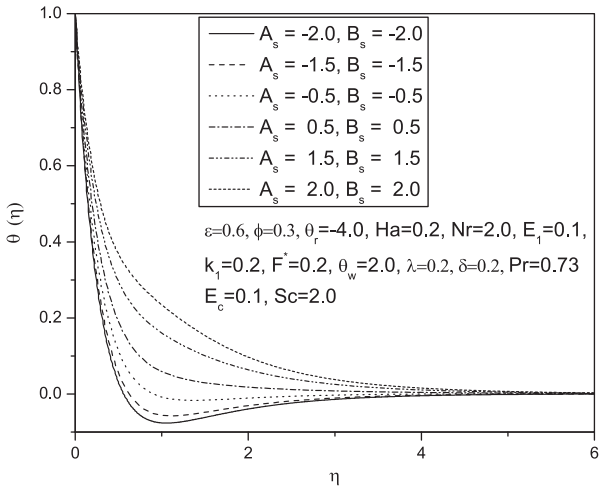

Figure 6 Effect of A_s,B_s on temperature profiles in PST case.

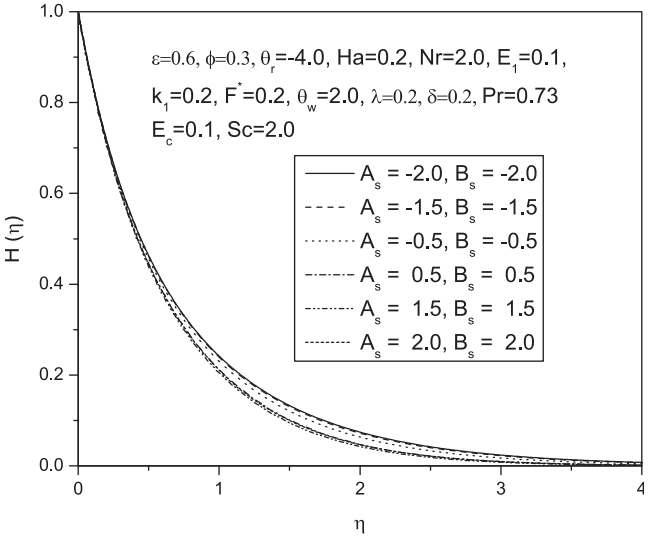

Figure 7 Effect of A_s,B_s on concentration profiles in PST case.

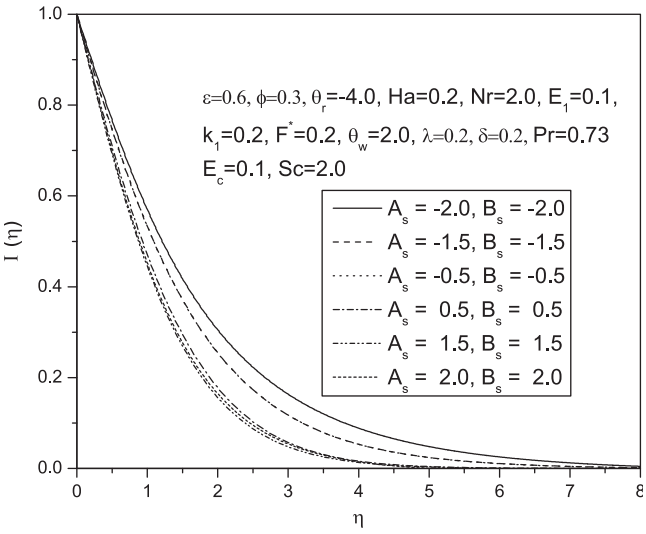

Figure 8 Effect on non-uniform heat source/sink parameter A_s, B_s on concentration profiles in PHF case.

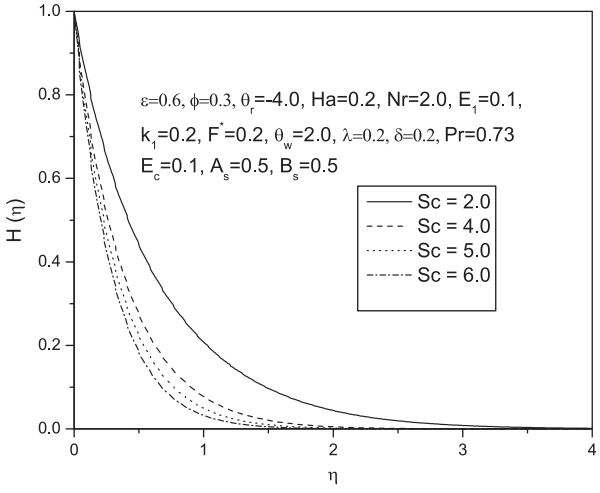

Figure 9 Concentration profile for different values of Schmidt number *Sc* in PST case.

case of A_s, $B_s < 0$ (absorbtion) the boundary layer releases energy resulting in the temperature profiles to decrease with increasing in the value of A_s,B_s in the thermal boundary layer.

Figs. 7 and 8 depict the effect of non-uniform internal heat generation A_s, $B_s > 0$ or absorption A_s, $B_s < 0$ in the boundary layer on the concentration field on $H(\eta)$ and $I(\eta)$ in PST and PHF cases respectively. It is observed that the concentration profiles decreases by increasing the values of A_s, $B_s > 0$ (heat source) whereas reverse trend is seen on concentration profiles by increasing the values of A_s, $B_s < 0$ (heat sink).

Figs. 9 and 10 exhibit the variation concentration profiles with η for different values of Schmidt number *Sc* in PST and PHF cases, respectively. It is observed that the effect of increasing the value of Schmidt number is to decrease the concentration of the diffusive species in both PST and PHF cases. Reduction in the concentration of diffusion species due to increase in the Schmidt number can be demonstrated by replacing hydrogen by water vapor and ammonia etc. in the said sequence for both PST and PHF cases.

Figs. 11–13 are the plots of local skin friction coefficient, local Nusselt number and local Sherwood number for various values of physical parameter such as $\epsilon = 0.6$, $\phi = 0.3$, $Ha = 0.2$, $Nr = 2.0$, $E_1 = 0.1$, $k_1 = 0.2$, $F^* = 0.2$, $\lambda = 0.2$, $E_1 = 0.1$,$\theta_r = -4.0$, θ_w2.0. Fig. 11 depicts the variation in the local skin-friction coefficient with Prandtl number *Pr* for various values of A_s, B_s. It is observed from this figure that the local skin-friction coefficient is increase due to increase in the A_s, $B_s > 0$, whereas reverse effect is seen on local skin-friction by increasing the Prandtl number. Figs. 12 and 13 describe the behavior of local Nusselt number and the local Sherwood number with changes in the values of A_s, B_s for different values of *Pr*. It is observed that the effect of increasing the value of A_s, B_s is to increase the local Nusselt number and decrease the local Sherwood number, whereas the effect of increase in the Prandtl number is to decrease in the value of local Nusselt number and local Sherwood number. The effect of Prandtl

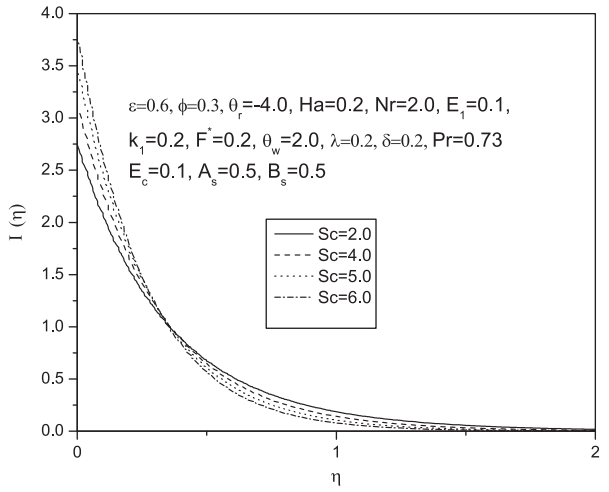

Figure 10 Concentration profile for different values of Schmidt number *Sc* in PHF case.

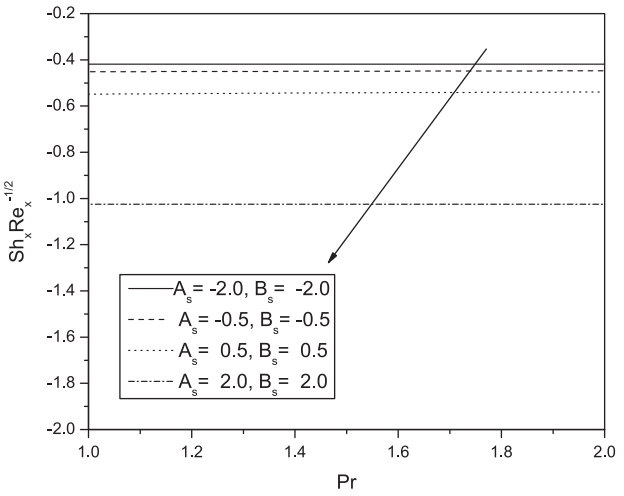

Figure 13 Local Sherwood number versus *Pr* for various of A_s, B_s.

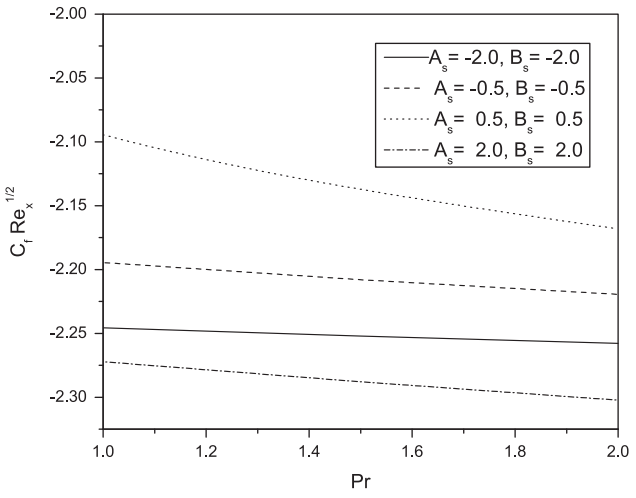

Figure 11 Local skin friction coefficient versus *Pr* for various of A_s,B_s.

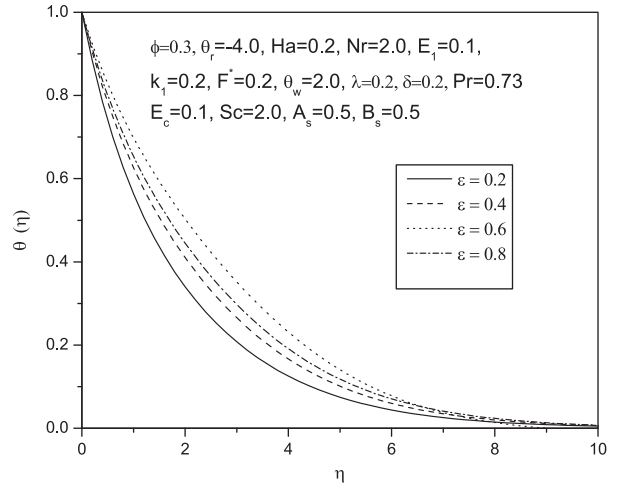

Figure 14 Effect of thermal conductivity parameter ϵ on temperature profile.

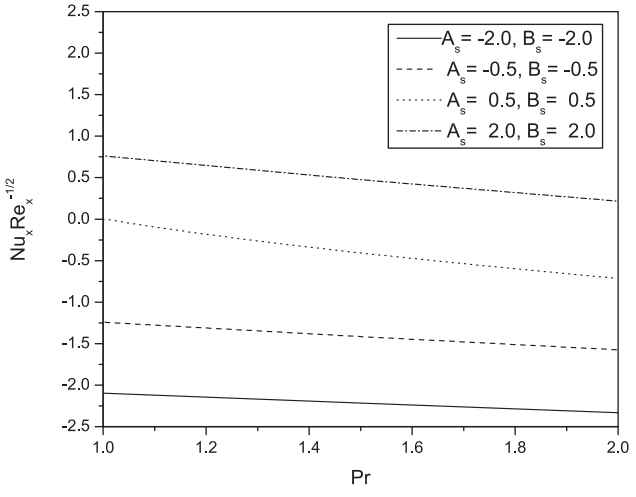

Figure 12 Local Nusselt number versus *Pr* for various of A_s, B_s.

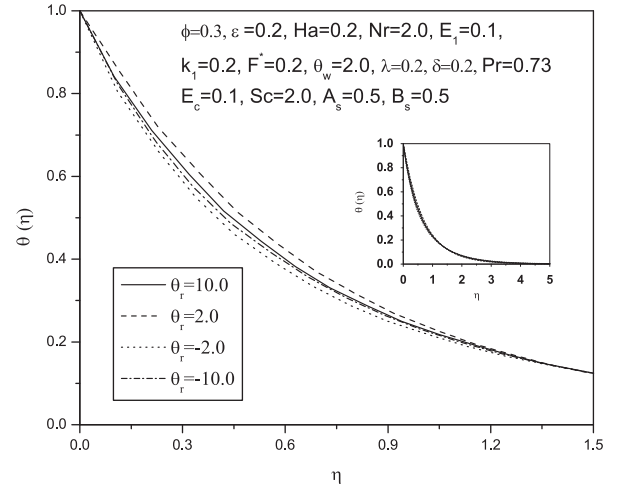

Figure 15 Effect of viscosity parameter θ_r on temperature profile in PST case.

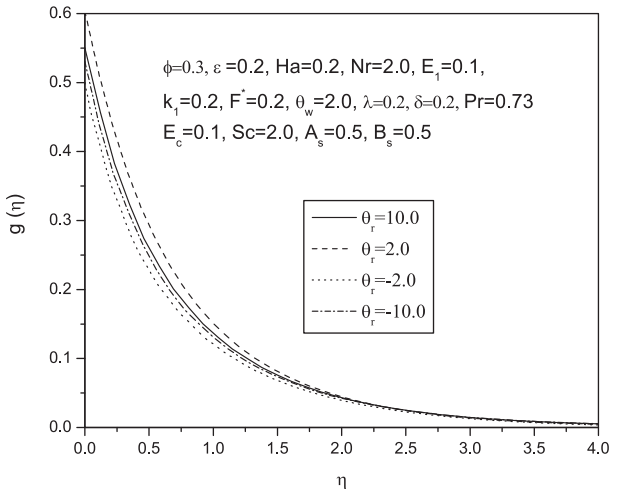

Figure 16 Effect of viscosity parameter θ_r on temperature profile in PHF case.

number is not much significant on the behavior of the Sherwood number.

The effect of variable thermal conductivity parameter ϵ on temperature profiles is shown in Fig. 14. It is observed from this plot that increasing the value of ϵ results in increasing the magnitude of temperature due to increase in the thermal boundary layer thickness. Figs. 15 and 16 display results for temperature distribution for various values of viscosity parameter θ_r in the boundary layer for PST and PHF cases, respectively. It is seen from these figures that the temperature decreases very rapidly with η and its value decreases with increase in θ_r. Similar trend is seen in the nature of the temperature profiles when temperature decreases with increase in the value of θ_r. Further, it is observed that the decrease in the temperature with θ_r is remarkable new to the stretching sheet.

5. Conclusions

The flow and heat mass transfer for a non-Darcy hydromagnetic flow over a stretching sheet submerged in a viscous fluid -saturated porous medium in the presence of a uniform transverse magnetic field are solved in this study. The resulting partial differential equations were transformed to a set of ordinary differential equations and then these equations are solved numerically using Runge–Kutta–Fehlberg method with shooting techniques. Graphical mode of presentation of the computed results illustrate the details of mass transfer characteristics and their dependence on some physical parameters. The important findings of our analysis are listed below:

(i) Increase in the Schmidt number Sc is to decrease the concentration profile in both PST and PHF cases.
(ii) The effect of non-uniform and temperature dependent heat source/sink parameters A_s, B_s leads to increase in the temperature profile.
(iii) The presence of space-dependent heat source/sink parameter A_s, B_s is to decrease the concentration profile in both PST and PHF cases.
(iv) The effect of buoyancy parameter is to increase the velocity distribution in the momentum boundary layer.
(v) Thermal boundary layer thickness decreases due to increase in buoyancy parameter λ.
(vi) The effect of porous parameter is to decrease velocity and increase temperature profiles throughout the momentum and thermal boundary layer, respectively.
(vii) Thermal boundary layer thickness increases due to increase in the variable thermal conductivity parameter ϵ.
(ix) The temperature profiles decreases very rapidly with decreases in θ_r in both PST and PHF cases.

References

[1] E.M. Sparrow, L. Lee, Analysis of mixed convection about a horizontal cylinder, Int. J. Heat Mass Transfer 19 (1976) 229–232.
[2] M.E. Ali, The effect of variable viscosity on mixed convection heat transfer along a vertical surface in a saturated porous medium, Int. J. Thermal. Sci. 45 (2006) 60–69.
[3] D. Pal, H. Mondal, Influence of temperature-dependent viscosity and thermal radiation on MHD forced convection over a non-isothermal wedge, Applied Mathematics and Computation 212 (2009) 194–208.
[4] D.A. Nield, A. Bejan, Convection in Porous Media, second ed., Springer-Verlag, New York, 1998.
[5] M. Abel, N. Mahesha, Heat transfer in MHD viscoelastic fluid flow over a stretching sheet with variable thermal conductivity, non-uniform heat source and radiation, Appl. Math. Model. 32 (2008) 1965–1983.
[6] C.K. Chen, C.R. Lin, Natural convection from an isothermal vertical surface embedded in a thermally stratified high-porosity medium, Int. J. Eng. Sci. 33 (1995) 131–138.
[7] T.W. Tong, E. Subramanian, Boundary layer analysis for natural convection in porous enclosure: use of the Brinkmann-extended Darcy model, Int. J. Heat Mass Transfer 28 (1985) 563–571.
[8] C.L. Tien, M.L. Hunt, Boundary-layer flow and heat transfer in porous beds, Chem. Eng. Progr. 21 (1987) 53–63.
[9] P. Singh, K. Tewari, Non-Darcy free convection from vertical surfaces in thermally stratified porous medium, Int. J. Eng. Sci. 31 (1993) 1233–1242.
[10] S. Kazem, M. Shaban, S. Abbasbandy, Improved analytical solutions to a stagnation-point flow past a porous stretching sheet with heat generation, J. Franklin Inst. 348 (2011) 2044–2058.
[11] Z. Uddin, M. Kumar, Effect of temperature dependent properties on MHD free convection flow and heat transfer near the lower stagnation point of a porous isothermal cylinder, Math. Phys. Comput. Modell. 13 (4) (2009) 15–20.
[12] K. Vajravelu, K.V. Prasad, C.O. Ng, Unsteady convective boundary layer flow of a viscous fluid at a vertical surface with variable fluid properties, Non Anal. Real World Appl. 14 (2013) 455–464.
[13] S. Mukhopadhyay. Effects of thermal radiation and variable fluid viscosity on stagnation point flow past a porous stretching sheet. Meccanica, doi:10.1007/s11012-013-9704-0.
[14] M. Mahantesh, K. Nandeppanavar, K. Vajravelu, M. Subhas Abel, M.N. Siddalingappa, MHD flow and heat transfer over a stretching surface with variable thermal conductivity and partial slip. Meccanica, http://dx.doi.org/10.1007/s11012-012-9677-4.
[15] M.M. Ali, T.S. Chen, B.F. Armaly, Natural convection–radiation interaction in boundary-layer flow over horizontal surfaces, AIAA J. 22 (1984) 1797–1803.
[16] D. Pal, Heat and mass transfer in stagnation-point flow towards a stretching surface in the presence of buoyancy force and thermal radiation, Meccanica 44 (2009) 145–158.

[17] R.C. Bataller, Radiation effects in the Blasius flow, Appl. Math. Comput. 198 (2008) 333–338.
[18] E. Magyari, A. Pantokratoras, Note on the effect of thermal radiation in the linearized Rosseland approximation on the heat transfer characteristics of various boundary layer flows, Int. Commun. Heat Mass Transfer 38 (2011) 554–556.
[19] D. Pal, H. Mondal, Effect of variable viscosity on MHD non-Darcy mixed convective heat transfer over a stretching sheet embedded in a porous medium with non-uniform heat source/sink, Commun. Nonlinear Sci. Numer. Simulat. 15 (2010) 1553–1564.
[20] S.M.M. EL-Kabeir, Soret and Dufour effects on heat and mass transfer by mixed convection over a vertical surface saturated porous medium with temperature dependent viscosity, Int. J. Numer. Methods Fluids 69 (10) (2012) 1633–1645.
[21] A. Aziz, F. Khani, Convection radiation from a continuously moving fin of variable thermal conductivity, J. Franklin Inst. 348 (2011) 640–651.
[22] M.E. Ali, The effect of variable viscosity on mixed convection heat transfer along a vertical moving surface, Int. J. Thermal. Sci. 45 (2006) 60–69.
[23] M. Hussain, M. Ashraf, S. Nadeem, M. Khan, Radiation effects on the thermal boundary layer flow of a micropolar fluid towards a permeable stretching sheet, J. Franklin Inst. 350 (2013) 194–210.
[24] M.A. Aziz, Temperature dependent viscosity and thermal conductivity effects on combined heat and mass transfer in MHD three-dimensional flow over a stretching surface with Ohmic heating, Meccanica 42 (2007) 375–386.
[25] G.K. Ramesh, B.J. Gireesha, C.S. Bagewadi, MHD flow of a dusty fluid near the stagnation point over a permeable stretching sheet with non-uniform source/sink, Int. J. Heat Mass Transfer 55 (2012) 17–18.
[26] R. Sivaraj, B. Rushi Kumar, Viscoelastic fluid flow over a moving vertical cone and flat plate with variable electric conductivity, Int. J. Heat Mass Transfer 61 (2013) 119–128.
[27] T.Y. Na, Computational Method in Engineering Boundary Value Problems, Academic Press, New York, 1979.
[28] E.C. Lai, F.A. Kulacki, Effects of variable viscosity on connective heat transfer along a vertical surface in a saturated porous medium, Int. J. Heat Mass Transfer 33 (1990) 1028–1031.
[29] D. Pal, H. Mondal, MHD non-Darcian mixed convection heat and mass transfer over a non-linear stretching sheet with SoretDufour effects and chemical reaction, Int. Commun. Heat Mass Transfer 38 (2011) 463–467.
[30] L. J Grubka, K.M. Bobba, Heat transfer characteristics of a continuous stretching surface with variable temperature, ASME J. Heat Transf. 107 (1985) 248–250.